Journal of Alzheimer's Disease 66 (2018) 307–318
DOI 10.3233/JAD-180360
IOS Press

Amyloid and FDG PET of Successful Cognitive Aging: Global and Cingulate-Specific Differences

Timothy M. Baran[a,*] and Feng Vankee Lin[b] for the Alzheimer's Disease Neuroimaging Initiative[1]
[a]*Departments of Imaging Sciences and Biomedical Engineering, University of Rochester, Rochester, NY, USA*
[b]*University of Rochester, School of Nursing, and Departments of Neuroscience, Neurology, Psychiatry, and Brain and Cognitive Sciences, Rochester, NY, USA*

Handling Associate Editor: Bernard Hanseeuw

Accepted 10 August 2018

Abstract.
Background: Some individuals, called Supernormals (SN), maintain excellent memory in old age. While brain structural and functional integrity in SN seem to be aging-resistant, their amyloidosis and neural injury status has not been well studied.
Objective: The goal of this study was to compare cortical amyloid deposition and glucose metabolism between SN and older adults with normal cognition (NC), amnestic mild cognitive impairment (MCI), and Alzheimer's disease (AD).
Methods: Subjects from the ADNI database were included if they received T1-weighted MRI, amyloid PET, FDG-PET, and cognitive testing within a 6-month period, yielding 27 AD, 69 MCI, 172 NC, and 122 SN. PET standardized uptake value ratios (SUVrs) were calculated for the whole cortex and 68 regions of interest, with whole cerebellum serving as reference.
Results: SN had lower whole cortex amyloid than MCI, and higher glucose metabolism than all others. Regional analysis revealed that amyloid burden and glucose metabolism in the right isthmus cingulate cortex differed in SN compared to others, while SN glucose metabolism also differed from others in several frontal and temporal regions.
Conclusion: Preserved cortical glucose metabolism, and lower levels of amyloidosis and glucose hypometabolism in the right isthmus cingulate cortex, contributes to the Supernormal phenomenon. These findings may be informative for development of early screening biomarkers and therapeutic targets for modification of cognitive trajectories.

Keywords: Amyloid-β, glucose metabolism, magnetic resonance imaging, positron emission tomography, successful cognitive aging, supernormal

INTRODUCTION

Descriptions of cognitive aging often assume deterioration of cognitive performance. However, some older adults maintain excellent memory capacity in advanced old age [1], with superior memory compared to age- and sex-matched counterparts [2, 3] or relative to normal middle-aged [4, 5] or younger adults [6, 7]. These older adults are considered "Superagers" or "Supernormals," with Superagers normally defined as those with comparable cognitive capacity to younger adults and

[1]Data used in preparation of this article were obtained from the Alzheimer's Disease Neuroimaging Initiative (ADNI) database (http://adni.loni.usc.edu). As such, the investigators within the ADNI contributed to the design and implementation of ADNI and/or provided data but did not participate in analysis or writing of this report. A complete listing of ADNI investigators can be found at: http://adni.loni.usc.edu/wp-content/uploads/how_to_apply/ADNI_Acknowledgement_List.pdf.

*Correspondence to: Timothy M. Baran, PhD, University of Rochester Medical Center, 601 Elmwood Ave, Box 648, Rochester, NY 14642, USA. Tel.: +1 585 276 3188; Fax: +1 585 273 1033; E-mail: Timothy.Baran@Rochester.edu.

Supernormals as those with superior cognitive capacity to older adults of similar age and education. In addition to superior memory, these Supernormal subjects also exhibit a lower frequency of the apolipoprotein E (ApoE) $\varepsilon 4$ allele [8] and lower levels of oxidative stress [3].

Recent longitudinal studies [9], including ours [10], suggest that brain structural and functional integrity in Supernormals seem to be aging-resistant. In particular, the cingulate cortex appears to play a critical role in the preservation of excellent memory in Supernormals [2, 8, 11]. Compared to their normal counterparts, Supernormals tend to have preserved cortical thickness in the anterior midcingulate cortex [6].

Cerebral amyloidosis and neural injuries, two main cognitive aging-related pathophysiological factors, are known to occur earlier than brain structural or functional deficits [12]. However, relatively few studies have investigated whether Supernormals display resistance to these pathophysiological changes in their aging process. Dekhtyar et al. demonstrated no difference in whole-cortex amyloid burden via positron emission tomography (PET) between "typical" and "optimal" memory performers [9]. Similarly, Harrison et al. found no difference in amyloid burden between successful agers and typical older adults, despite changes in cortical thickness [7]. Gefen et al. showed a lower frequency of Alzheimer-type neurofibrillary tangles in Superagers than their age-matched counterparts [11]. However, no study has directly compared both cerebral amyloidosis and neural injuries in Supernormals.

Here, we compared amyloid and fluorodeoxyglucose (FDG) PET between Supernormals and other typical or symptomatic aging groups [average agers, amnestic mild cognitive impairment (MCI), Alzheimer's disease (AD)]. Amyloid PET was used as an indicator of amyloidosis, while FDG-PET, reflecting synaptic dysfunction, served as a neural injury maker. We hypothesized that Supernormals would display comparable amyloid burden to typical agers, while showing differences in glucose metabolism. Based on our prior studies [2], we expected these effects to be particularly pronounced in the cingulate cortex.

MATERIALS AND METHODS

Data source

Data used in the preparation of this article were obtained from the Alzheimer's Disease Neuroimaging Initiative (ADNI) database (http://adni.loni.usc.edu). The ADNI was launched in 2003 as a public-private partnership, led by Principal Investigator Michael W. Weiner, MD. The primary goal of ADNI has been to test whether serial magnetic resonance imaging (MRI), PET, other biological markers, and clinical and neuropsychological assessment can be combined to measure the progression of MCI and early AD. For up-to-date information, see http://www.adni-info.org.

Participants and cognitive assessments

All data were acquired from the ADNIGO and ADNI2 datasets. Both AD and MCI subjects had Wechsler Memory Scale Logical Memory II scores $\leq$8 for those with 16+ years of education, $\leq$4 for 8-5 years of education, and $\leq$2 for less than 7 years of education. AD subjects had a Mini-Mental State Exam (MMSE) score of 20–26 and Clinical Dementia Rating (CDR) of 0.5 or 1. MCI subjects had a MMSE score of 26–30 and CDR of 0.5. Average agers/normal controls (NC) and supernormal (SN) subjects were identified as those free of MCI, any types of dementia, and major psychiatric disorders, as well as having a MMSE score 24–30, CDR of 0, and Wechsler Memory Scale Logical Memory II scores >8 for those with 16+ years of education, >4 for 8–15 years of education, and >2 for less than 7 years of education. SN subjects were separated from NC based on a latent class approach, which identified those who displayed constantly high, stable episodic memory and executive function over a 5-year period compared to age- and education-matched controls, as described previously [1]. These SN subjects had baseline episodic memory (ADNI-MEM) and executive function (ADNI-EF) mean z-scores of 1.51 and 1.05, respectively, compared to 1.0 ± 0.5 and 0.7 ± 0.67 for cognitively normal subjects in the ADNI sample [13, 14]. These are approximately 1 standard deviation above the overall normal population mean, indicating that this SN group is at or above 84% of the population, assuming cognitive scores are normally distributed. Furthermore, the mean slope of cognitive trajectories for SN subjects was positive over a 5-year period, whereas cognitively normal subjects had a negative slope. To ensure comparability with our previous fMRI study [10], we used the same sample pool (354 SN+NC subjects, 98 MCI+AD subjects). Subjects were required to have T1-weighted MR imaging, amyloid PET imaging, FDG-PET imaging, and

cognitive testing within a 6-month period. The final sample included 27 AD, 69 MCI, 172 NC, and 122 SN individuals.

Memory performance was scored using the ADNI-MEM composite, which consists of the Rey Auditory Verbal Learning Test, Alzheimer's Disease Assessment Scale-Cognition subscale, Mini-Mental State Examination, and Logical Memory test [13]. Executive function was scored using the ADNI-EF composite, which includes WAIS-R Digit Symbol Substitution, Digit Span Backwards, Trails A and B, Category Fluency, and Clock Drawing [14]. The Montreal Cognitive Assessment (MOCA) score was used to assess global cognition [15]. Whereas the SN group was defined based on cognitive trajectories, the MEM, EF, and MOCA scores analyzed in the current study were from a single time point that fell within 6 months of the desired T1-weighted MR, amyloid PET, and FDG-PET imaging.

Imaging and image analysis

All subjects received structural T1-weighted MR imaging using a 3.0 T scanner, with a magnetization-prepared rapid gradient-echo (MPRAGE) sequence. PET imaging was performed with 2 tracers: AV45 (^{18}F florbetapir, Amyvid, Eli Lilly and Company, Indianapolis, IN) for amyloid and 2-deoxy-2-[fluorine-18]-D-glucose (^{18}F FDG) for FDG-PET. Pre-processed T1 images were acquired from the ADNI database, including gradient warping, scaling, B1 correction, and N3 inhomogeneity correction. PET images were downloaded in their fully pre-processed form (Coreg, Avg, Standardized Image and Voxel Size) for both tracers.

T1 images were segmented using FreeSurfer 5.3.0 (http://surfer.nmr.mgh.harvard.edu). Following automated segmentation, results were examined by eye for topological defects, with manual correction performed whenever necessary. Cortical thickness measurements were extracted from these corrected Freesurfer results. Thickness was analyzed rather than volume, as this has been shown to be less sensitive to confounding factors such as sex and head size [16]. T1 images were then registered to the MNI152 template at an isotropic resolution of 3 mm (MNI152_T1_2 mm downsampled to 3 mm) using FMRIB's Linear Image Registration Tool with 12 degrees of freedom (FLIRT, FSL 5.0.10, http://fsl.fmrib.ox.ac.uk). For each subject, this transformation was then applied to segmented images in order to translate ROIs to template space. Amyloid PET images were co-registered to these T1 images in MNI152 space, using FLIRT. FDG-PET images were registered to a PET template in MNI space [17] at an isotropic resolution of 3 mm using FLIRT. All analyses were performed in MNI template space, in order to allow for direct visualization of mean values across subjects. The standardized uptake value ratio (SUVr) was calculated for each PET voxel, with the reference region set to the whole cerebellum. SUVrs were extracted from all 68 cortical ROIs identified by Freesurfer (Desikan-Killiany atlas [18]) in MNI space, and averaged to produce a cortical summary SUVr, due to reports of non-specific binding of AV45 in the white matter [19]. Mean SUVrs were also calculated for the 68 ROIs extracted by FreeSurfer in MNI space. PET results were not corrected for partial volume effects, in order to replicate the analysis described by the ADNI PET Core [20, 21].

In addition to the continuous SUVr values for amyloid and FDG-PET, we further examined the subsample of SN and NC ($n = 292$) for amyloid and neural injury positivity, as these binarized biomarkers have recently been identified as potential diagnostic criteria for AD [22]. We defined amyloid positive (A+) and negative (A–) subjects based on a cutoff point of 1.11 in amyloid cortical summary SUVr [23], corresponding to the confidence limit for the upper 5% of young healthy controls [24]. Neural injury positive (N+) and negative (N–) subjects were defined based on a cutoff point of 1.21 in AD-signature FDG-PET SUVr, which was initially chosen to separate control and AD subjects in the ADNI database [25]. Both of these sets of summary SUVr values were generated by the ADNI PET Core, as described online [20, 21]. We extracted these values from publicly available results, and applied the above thresholds to separate subjects into 4 groups (A+N+, A+N–, A–N+, A–N–).

Statistical analysis

ANOVA, chi-square test, or ANCOVA (when controlling for covariates) were used to examine group differences in demographic characteristics, PET values, cortical thicknesses, and cognitive scores, with *post hoc* testing performed comparing SN with other groups. False discovery rate (FDR) correction was applied. All statistical analyses were performed in SPSS (IBM Corp, Armonk, NY) and MATLAB (The MathWorks, Inc, Natick, MA).

RESULTS

Sample characteristics

Subject characteristics across groups are presented in Table 1. The SN group was significantly older than the MCI group, and was more educated and had fewer APOE4+ carriers than the AD group. The SN group had significantly higher ADNI-MEM, ADNI-EF, and MOCA scores compared to all other groups, and significantly higher whole brain cortical thickness than AD and MCI groups. For the overall ADNI sample, cognitively normal individuals have mean ADNI-MEM of 1.0 ± 0.5 and ADNI-EF of 0.7 ± 0.67 [13, 14]. In contrast, the SN group has a mean ADNI-MEM of 1.46 ± 0.49 and ADNI-EF of 1.22 ± 0.68. Both of these are approximately 1 standard deviation above the overall normal population mean, indicating that this SN group is at or above 84% of the population. On the other hand, the NC group has ADNI-MEM and ADNI-EF scores of 0.92 ± 0.54 and 0.50 ± 0.64, respectively. Further, in order to ensure that our NC and SN subjects were representative of the overall ADNI sample in terms of memory performance and executive function, we grouped NC+SN together and compared to all cognitively normal subjects in ADNI. Neither ADNI-MEM nor ADNI-EF were significantly different from cognitively normal subjects in the overall ADNI sample (ADNI-MEM: Mean diff. (MD) = –0.05, std. error (SE) = 0.04, $t = 1.20$, $p = 0.23$; ADNI-EF: MD = 0.08, SE = 0.06, $t = 1.38$, $p = 0.17$).

Amyloid PET imaging

Group differences in amyloid SUVr for the whole cortex are given in Table 1, and are displayed in Fig. 1a. The four groups significantly differed in whole cortex amyloid SUVr. Controlling for age, sex, APOE4, education, and whole brain cortical thickness, the group difference remained ($F = 14.10$, df1 = 3, df2 = 394, $p < 0.001$). The SN group had significantly lower amyloid SUVr than the MCI (MD = –0.08, SE = 0.03, $t = 2.96$, df = 187, $p = 0.003$) and AD (MD = –0.24, SE = 0.04, $t = 6.21$, df = 147, $p < 0.0001$) groups. In order to reduce the potential effects of noise at low SUVr values on these results, we additionally performed this analysis while excluding cases with SUVr less than 1. Similar results were observed for both the SN versus MCI (MD = –0.09, SE = 0.03, $p = 0.003$) and SN versus AD comparisons (MD = –0.22, SE = 0.04, $p < 0.0001$).

Regional differences in PET signal were compared in 68 cortical ROIs using ANOVA, controlling for age, sex, APOE4, education, and cortical thickness within the corresponding ROI. For all regions in which there were significant group differences, amyloid SUVrs were contrasted against SN values. After FDR correction was applied across the results of these contrast tests, the right isthmus cingulate cortex was found to have significantly lower AV45 uptake in SN subjects compared to NC (MD = –0.05, SE = 0.02, $t = 2.34$, df = 295, $p = 0.020$), MCI (MD = –0.09, SE = 0.03, $t = 2.72$, df = 184, $p = 0.007$), and AD (MD = –0.22, SE = 0.05, $t = 4.60$, df = 145, $p < 0.0001$), as shown in Fig. 1b. As above, exclusion of SUVr values less than 1 gave similar results for all comparisons (NC: MD = –0.05, SE = 0.02, $p = 0.049$; MCI: MD = –0.09, SE = 0.03, $p = 0.005$; AD: MD = –0.22, SE = 0.05, $p < 0.0001$).

FDG-PET imaging

Whole cortex results are presented in Table 1 and Fig. 2a. FDG uptake in the SN group was significantly different from all other groups. Controlling for age, sex, APOE4, education, and whole brain cortical thickness, the group difference remained ($F = 31.19$, df1 = 3, df2 = 405, $p < 0.001$). The SN group had significantly higher SUVr than the NC (MD = 0.03, SE = 0.01, $t = –2.06$, df = 315, $p = 0.040$), MCI (MD = 0.06, SE = 0.02, $t = –3.59$, df = 191, $p < 0.0001$) and AD (MD = 0.25, SE = 0.03, $t = –9.45$, df = 151, $p < 0.0001$) groups after controlling for these factors.

The procedure described above for comparison of ROI differences was also applied to FDG-PET. After FDR correction, a number of ROIs were shown to have significant differences between SN and other groups, as highlighted in Fig. 2c and Table 2 for the NC to SN comparison. In particular, the right isthmus cingulate cortex also showed significance in the case of FDG-PET between SN and NC (MD = 0.04, SE = 0.02, $t = –1.97$, df = 315, $p = 0.043$), MCI (MD = 0.09, SE = 0.03, $t = –3.39$, df = 183, $p = 0.001$), and AD (MD = 0.24, SE = 0.04, $t = –6.22$, df = 148, $p < 0.0001$), as shown in Fig. 2b.

Synthesizing amyloid and FDG-PET

In order to investigate the possible influence of amyloidosis on hypometabolism, and vice versa, the above analyses were repeated while controlling for uptake of the opposite radiotracer. When

Table 1
Sample characteristics

	AD ($n=27$)	MCI ($n=69$)	NC ($n=172$)	SN ($n=122$)[#]	F or χ^2 test, df (p)
Age, M ± SD	73.18 ± 7.34	71.27 ± 7.84*	74.56 ± 6.17	73.88 ± 6.64	4.17, 3, 424 (0.006)
Male, *n* (%)	13 (50.0)	35 (53.0)	102 (52.3)	50 (36.5)	9.32, 3 (0.025)
Years of education, M ± SD	15.15 ± 2.51**	16.23 ± 2.68	16.48 ± 2.69	16.88 ± 240	3.59, 3, 421 (0.014)
APOE4+, *n* (%)	20 (76.9)*	30 (44.1)*	59 (30.1)	31 (22.8)	33.71, 3 (<0.001)
MEM, M ± SD	–0.98 ± 0.51***	0.36 ± 0.61***	0.92 ± 0.54***	1.46 ± 0.49	131.96, 3, 400 (<0.001)[†]
EF, M ± SD	–0.88 ± 0.70***	0.41 ± 0.93***	0.50 ± 0.64***	1.22 ± 0.68	54.50, 3, 400 (<0.001) †
MOCA, M ± SD	16.8 ± 5.52***	23.4 ± 3.17***	24.9 ± 2.52***	26.6 ± 2.33	82.49, 3, 385 (<0.001)
Whole brain cortical thickness (mm), M ± SD	2.17 ± 0.11***	2.32 ± 0.10***	2.27 ± 0.12	2.29 ± 0.11	10.62, 3, 417 (<0.001)
Whole cortex AV45 PET (SUVr), M ± SD	1.45 ± 0.19***	1.18 ± 0.19	1.11 ± 0.18	1.08 ± 0.13	27.76, 3, 409 (<0.001)
Whole cortex FDG PET (SUVr), M ± SD	1.04 ± 0.12***	1.28 ± 0.12***	1.30 ± 0.12**	1.34 ± 0.10	50.12, 3, 422 (<0.001)

Note. [#]All *post-hoc* analyses were based on comparison of SN with each of the other groups, FDR correction applied. [†]MEM and EF comparisons were controlled for the number of times subjects had previously performed MEM/EF testing, in order to correct for practice effects. *$p<0.05$; **$p<0.01$; ***$p<0.001$.

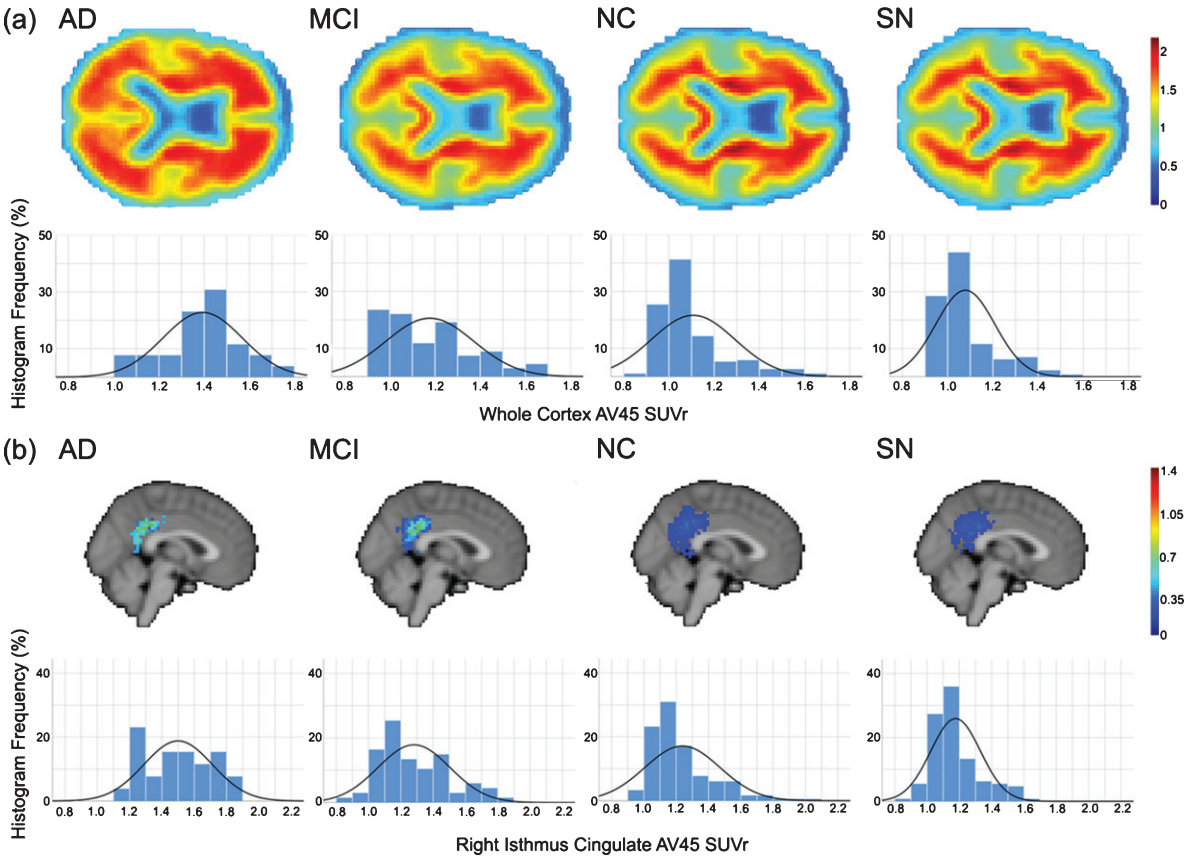

Fig. 1. (a) Axial views and SUVr histograms for whole brain mean amyloid PET SUVr, and (b) sagittal views and SUVr histograms for mean right isthmus cingulate amyloid PET SUVr for each of the diagnostic groups. SUVr values were normalized to the whole cerebellum, and are presented in the colorbars for mean images. Histograms indicate relative frequency for given SUVr values across all subjects, as a percentage of the total voxel values, in the corresponding region (a: whole brain; b: right isthmus cingulate). Solid curves are normal distributions fit to the histogram data.

controlling for whole cortex FDG, the group difference in whole cortex amyloid remained ($F=10.53$, $df1=3$, $df2=394$, $p<0.001$), with the SN group showing reduced amyloid burden compared to MCI (Mean diff. (MD) = –0.07, std. error (SE) = 0.03, $t=2.81$, $df=187$, $p=0.005$) and AD (MD = –0.23,

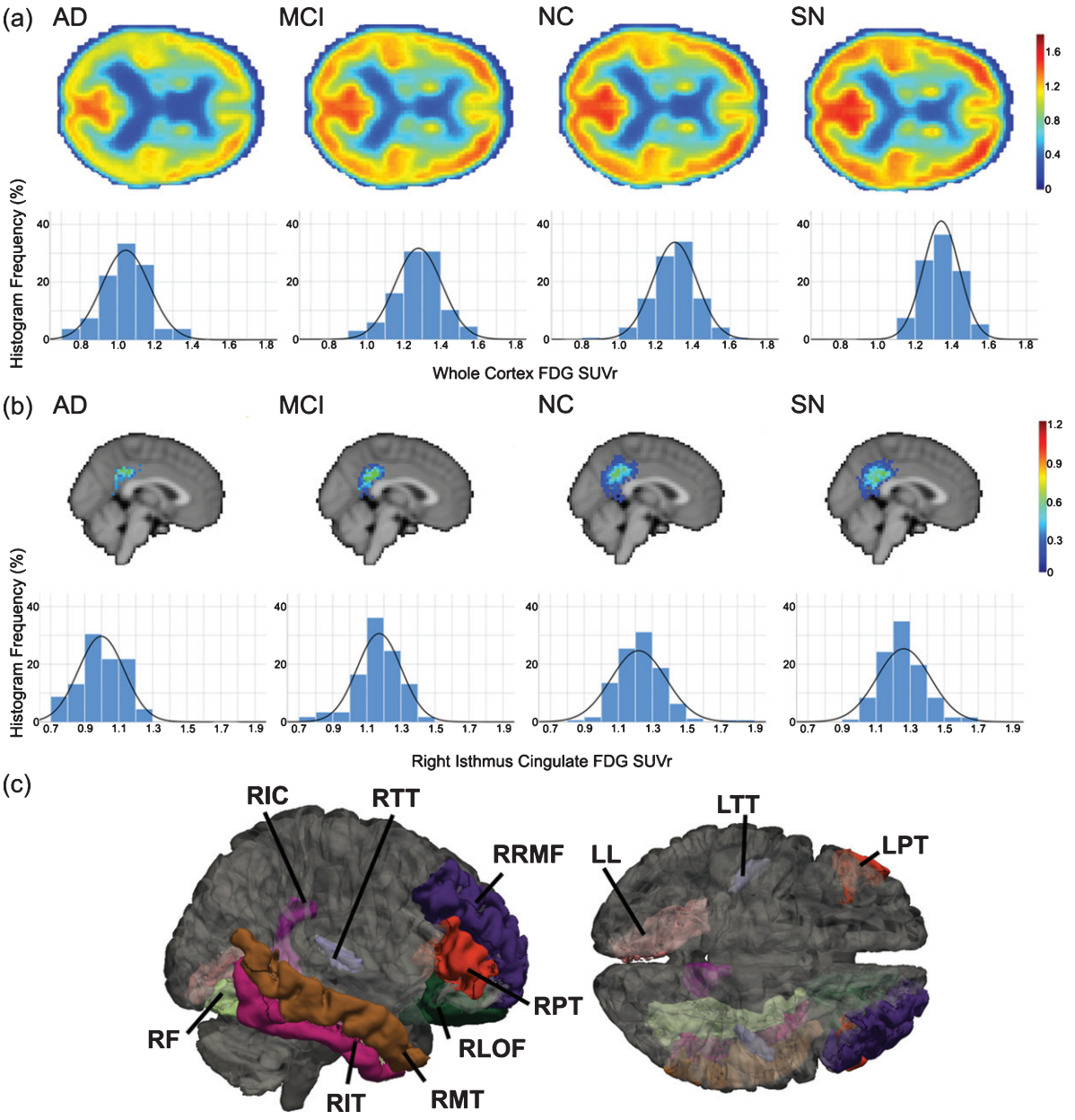

Fig. 2. (a) Axial views and SUVr histograms for whole brain mean FDG-PET SUVr, and (b) sagittal views and SUVr histograms for mean right isthmus cingulate FDG-PET SUVr for each of the diagnostic groups. SUVr values were normalized to the whole cerebellum, and are presented in the colorbars for mean images. Histograms indicate relative frequency for given SUVr values across all subjects, as a percentage of the total voxel values, in the corresponding region (a: whole brain; b: right isthmus cingulate). Solid curves are normal distributions fit to the histogram data. (c) ROIs showing significant differences in FDG-PET SUVr between NC and SN subjects. ROIs are right isthmus cingulate (RIC), right transverse temporal (RTT), right rostral middle frontal (RRMF), right pars triangularis (RPT), right lateral orbital frontal (RLOF), right middle temporal (RMT), right inferior temporal (RIT), right fusiform (RF), left lingual (LL), left transverse temporal (LTT), and left pars triangularis (LPT).

SE = 0.04, $t = 5.36$, df = 147, $p < 0.0001$) groups. FDG was not a significant predictor of whole cortex amyloid (B = –0.033, SE = 0.075, $t = -0.44$, df = 394, $p = 0.66$). This was also true for the right isthmus cingulate cortex, where SN subjects again showed significantly lower AV45 uptake compared to NC (MD = –0.05, SE = 0.02, $t = 2.25$, df = 295, $p = 0.025$), when controlling for FDG uptake in the right isthmus

Table 2
Regions of Interest showing significant differences in FDG-PET SUVr between NC and SN subjects

ROI	Hemisphere	Mean Difference (Std. Error)	t, df (p)[#]
Isthmus Cingulate	Right	0.035 (0.018)	2.43, 405 (0.040)[†]
Lingual	Left	0.034 (0.016)	2.60, 405 (0.029)
Pars Triangularis	Left	0.054 (0.024)	2.69, 402 (0.025)
	Right	0.059 (0.021)	3.29, 402 (0.006)[†]
Transverse Temporal	Left	0.049 (0.025)	2.52, 405 (0.035)
	Right	0.055 (0.023)	3.14, 405 (0.009)[†]
Fusiform	Right	0.030 (0.016)	2.38, 405 (0.044)
Inferior Temporal	Right	0.038 (0.016)	2.89, 405 (0.017)[†]
Lateral Orbital Frontal	Right	0.038 (0.020)	2.47, 405 (0.038)[†]
Middle Temporal	Right	0.033 (0.015)	2.52, 405 (0.035)[†]
Rostral Middle Frontal	Right	0.050 (0.021)	3.07, 402 (0.011)[†]

Note. [#]FDR correction applied. [†]Indicates significant difference after correction for amyloid SUVr in the same region.

cingulate. FDG was also not a significant predictor of amyloid in this case (B = 0.068, SE = 0.067, $t = 1.02$, df = 394, $p = 0.31$).

When controlling for amyloid uptake in the FDG analyses, whole cortex differences remained (F = 26.88, df1 = 3, df2 = 405, $p < 0.001$), with the SN group still displaying significantly higher SUVr than the NC (MD = 0.03, SE = 0.01, $t = -1.99$, df = 315, $p = 0.047$), MCI (MD = 0.06, SE = 0.02, $t = -3.37$, df = 191, $p = 0.001$) and AD (MD = 0.24, SE = 0.03, $t = -8.83$, df = 151, $p < 0.0001$) groups. As above, whole cortex amyloid was not a significant predictor of FDG (B = –0.031, SE = 0.032, $t = -0.96$, $p = 0.34$). At the regional level, correction for amyloid still resulted in a significant difference between SN and NC subjects in the right isthmus cingulate (MD = 0.03, SE = 0.02, $t = -1.86$, df = 315, $p = 0.048$), with amyloid again not a significant predictor (B = 0.002, SE = 0.049, $t = 0.036$, $p = 0.97$). However, some regions shown in Table 2 did not maintain significant differences between SN and NC subjects after applying this correction, as described in the footnote to the table.

Secondary analysis: SN versus NC in the context of AD-associated pathophysiology

To further understand whether differing levels of FDG uptake explained cognitive differences between SN and NC despite similar amyloid deposition, we examined the relationship between amyloid, FDG, and cognitive function within the subsample of SN and NC. SN subjects had 4 A+N+, 28 A+N–, 8 A–N+, and 81 A–N–, while NC had 15 A+N+, 47 A+N–, 16 A–N+, and 93 A–N–. More participants in the SN group were A–N– ($n = 81$, 66.9%) compared to the NC group ($n = 81$, 54.4%, $p = 0.039$), while the two groups were similar in other pathophysiology categories ($\chi^2 = 7.61$, df = 3, $p = 0.055$).

Next, we examined the main and interaction terms between group and FDG on MEM and EF when considering the effect of amyloid ($y_{MEM/EF} = \beta_0 + \beta_1 age + \beta_2 gender + \beta_3 MOCA + \beta_4 cortical\ thickness + \beta_5 group + \beta_6 AV45 + \beta_7 FDG + \beta_8\ FDG \times group$). Here, AV45 and FDG represent whole-cortex SUVr. There was a significant interaction effect between group and FDG on ADNI-MEM (B = 1.05, SE = 0.51, Wald's $\chi^2 = 4.18$, df = 1, $p = 0.041$) but not ADNI-EF after controlling for AV45 and other factors. There was no interaction effect between group and AV45 on MEM or EF after controlling for FDG and other factors. As shown in Fig. 3, this is indicative of a relationship between adjusted MEM score and whole cortex FDG for NC, but not for SN.

DISCUSSION

We previously identified a group of Supernormal subjects, based on high, sustained episodic memory and executive function [1, 10]. By examining their cognitive aging-associated pathophysiology, we found that: 1) whole cortex FDG-PET significantly distinguished SN from both typical and symptomatic agers. Whole cortex amyloid PET only distinguished SN from symptomatic agers (MCI and AD), but not typical agers; 2) for regional analyses, FDG-PET showed significant group differences in several prefrontal and inferior/middle temporal regions, while the right isthmus cingulate cortex was the only region across the 68 ROIS examined whose amyloid and FDG levels significantly distinguished SN from other groups; 3) when controlling for FDG uptake, all global and regional amyloid differences remained.

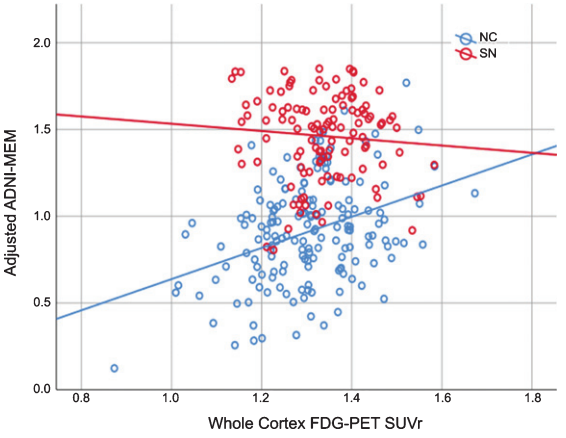

Fig. 3. Relationship between whole-cortex FDG-PET SUVr and adjusted ADNI-MEM score, for normal controls (NC) and Supernormals (SN). MEM score has been adjusted for age, sex, diagnostic group, mean cortical thickness, MOCA, and whole cortex amyloid SUVr. Solid lines are linear fits to data.

When FDG regional analyses were controlled for amyloid, the right isthmus cingulate still showed significant differences between SN and NC, though several previously identified regions did not. Further, amyloid level was not predictive of FDG, and vice versa, either globally or regionally; 4) despite similar levels of whole cortex amyloid deposition between SN and NC, individuals within the SN group had a higher probability of being both amyloid and neural injury negative than those in the NC group. When controlling for amyloid deposition, higher FDG level was related to higher memory performance in NC, while the SN group maintained high-level memory performance regardless of the level of FDG.

We examined main and interaction effects for amyloidosis and neural injury between SN and typical and symptomatic agers. Despite significant differences compared to MCI and AD, the lack of difference in global amyloid deposition between SN and NC corresponds with previous results [7, 9], where whole-cortex amyloid burden was similar between optimal or successful agers and typical memory performers. In the study by Dekhtyar et al., it should be noted that optimal memory performers that maintained memory over three years displayed lower levels of amyloid burden compared to those optimal memory performers that did not [9]. On the other hand, global FDG-PET was different between SN and all other groups. As part of the normal aging process, global reductions in metabolism have been observed, with hypometabolism particularly evident in medial frontal and frontal opercular areas [26]. Furthermore, the presence of both hypometabolism and amyloidosis accelerates AD conversion [27, 28]. While amyloid burden is typically correlated with reduced memory performance in normal individuals [29], amyloid burden was comparable between SN and NC. Separation in cognitive function between the two groups may therefore be primarily explained by differences in glucose metabolism. This finding is consistent with previous results showing the increased relevance of neurodegeneration for cognitive function compared to amyloidosis [16].

The next major finding is the critical role of the right isthmus cingulate cortex, whose amyloid burden and glucose metabolism level helped distinguish SN from other groups. Much of the neuroimaging literature related to memory deterioration in typical or symptomatic aging has focused on medial temporal/hippocampal and prefrontal disruptions [30, 31]. However, in the context of the Supernormal phenomenon, the cingulate cortex plays a unique role, with Supernormals displaying higher cortical thickness in the anterior [8, 11] and midcingulate cortex [6]. We have previously shown differences in the functional connectivity of multiple regions of the cingulate cortex, even in the presence of amyloid [2]. Combined with results showing reduced tau accumulation in the mid- and anterior cingulate cortex in Superagers [11], this points to the importance of the entire cingulate cortex as a potential "signature" region for superior performance in older adults. Different portions of this region may play different roles in the preservation of cognitive function, with amyloid deposition typically occurring early in the disease process in the posterior cingulate [32] and aging-related neurodegeneration becoming evident in anterior regions [33]. Thus, the observed maintenance of cortical thickness in the anterior and midcingulate and lower levels of amyloid/hypometabolism in the posterior cingulate for Supernormals/Superagers may represent two simultaneous mechanisms by which these individuals resist aging-related decline. Further studies are required to determine the causal relationship between these pathophysiological and structural changes, as this may either indicate increased neural reserve or compensation in this population [34]. An understanding of the mechanisms of cognitive reserve in relation to the Supernormal phenomenon could play an important role in the description of their neural profile.

In particular, the isthmus of the cingulate gyrus forms a connection between the posterior cingulate

cortex and the hippocampus, and is known to be part of the default mode network (DMN) [35, 36], which is the primary network affected in both normal aging and AD [37, 38]. The involvement of amyloid plaque was observed in this disruption of the DMN, especially the connection between the posterior cingulate cortex and the hippocampus, even in those without dementia [39]. FDG-PET studies have shown changes in the DMN in AD subjects [40], particularly in the posterior cingulate and precuneus. This was further verified by Liguori et al., who demonstrated glucose hypometabolism in DMN regions, including the cingulate [41]. Furthermore, these changes in metabolism were shown to correlate with altered functional connectivity [42], indicating an association between PET and fMRI measures of DMN aberration in AD-related aging. These studies point to the importance of the DMN, particularly posterior regions of the cingulate cortex, in maintenance of superior memory performance in advanced old age. The results of this study further reinforce this, as both amyloid and FDG-PET showed significant differences between normal and Supernormal subjects in the isthmus cingulate cortex.

Several studies have also demonstrated the synergistic effects of amyloid and tau pathology on hypometabolism, particularly within the cingulate cortex. Using amyloid, tau, and FDG-PET imaging, Hanseeuw et al. showed that global amyloid burden and inferior temporal tau predicted FDG metabolism in the posterior cingulate cortex [43]. Furthermore, Pascoal et al. found that only the interaction between amyloid and tau measures was a significant predictor of metabolic decline in multiple regions, including the posterior cingulate cortex [44]. Unfortunately, only a small number of the identified Supernormal subjects in the ADNI database have received tau PET imaging. While this sample size was insufficient for analysis in the current study, examination of the important role of tau pathology in the Supernormal phenomenon will be an important step in future studies.

The ultimate goal of research on AD-related aging is the translation of findings to disease-modifying therapy. Recently, the use of biomarkers has emerged as a potential outcome metric for clinical trials [45, 46]. While many drug trials have focused on advanced-stage patients [47–49], another area of focus has been on cognitive training for older adults that may be at risk for disease progression [50, 51]. This is particularly relevant in the context of normal versus Supernormal older adults, as we have previously demonstrated inducible neuroplasticity of the cingulate cortex [52], which has been shown to play an important role in successful aging. It remains to be seen whether these non-pharmacological trials can affect AD-related pathophysiology at a level evident via imaging biomarkers.

We acknowledge a number of limitations on the general applicability of the results demonstrated here. The first of these is selection bias in the ADNI sample that may skew the population studied. Second, the cross-sectional nature of the study precluded identification of whether the Supernormal phenomenon is determined by reserved cerebral metabolism. Third, the ROI analysis is vulnerable to some subjectivity in the correction of topological defects in the FreeSurfer segmentation, as this was performed manually. This may affect interpretation of the results related to the isthmus cingulate, as this is a relatively small region. Additionally, PET results were not corrected for partial volume effects, in order to replicate prior, well-characterized analyses and allow for inclusion of previously-defined thresholds for biomarker positivity. Investigation of the effects of partial volume correction merits future investigation. Although additional analyses performed excluding amyloid images with SUVr <1 did not modify the overall results, PET analysis may also be vulnerable to the effects of noise. This points to the need for development of more sensitive measures of amyloid deposition. Finally, the definitions of Supernormal, Superager, and successful ager are not standardized. This could cause results to change depending on which definition is applied to the subject population, and represents an ongoing area of discussion in the field. Here we have used a latent class approach for defining the SN group relative to an age- and education-matched group of cognitively healthy individuals, which may be challenging to apply in other subject cohorts. Based on the cognitive characteristics of SN in our studies [1, 2, 10], we suggest defining SN based on episodic memory greater than 1.5 standard deviations above the age- and education-matched population norm with longitudinal stability, while other cognitive domains (e.g., executive function) should be similar to or better than population norms with longitudinal stability.

In summary, we have demonstrated that global changes in glucose metabolism can distinguish Supernormals from both typical and symptomatic agers, while amyloid deposition only separates Supernormals from symptomatic agers. Both amyloid and glucose metabolism were different in SN from all others in the right isthmus cingulate

cortex. This reinforces the critical involvement of altered neural injury in successful cognitive aging, and the importance of the integrity of the default mode network in maintenance of memory performance in old age. These findings may be particularly informative for development of early screening biomarkers and therapeutic targets for modification of cognitive trajectories in the face of cognitive aging-associated pathophysiology.

ACKNOWLEDGMENTS

This study was supported by the National Institutes of Health (R01 NR015452).

Data collection and sharing for this project was funded by the Alzheimer's Disease Neuroimaging Initiative (ADNI) (NIH Grant U01 AG024904) and DOD ADNI (Department of Defense award number W81XWH-12-2-0012). ADNI is funded by the National Institute on Aging, the National Institute of Biomedical Imaging and Bioengineering, and through generous contributions from the following: AbbVie, Alzheimer's Association; Alzheimer's Drug Discovery Foundation; Araclon Biotech; BioClinica, Inc.; Biogen; Bristol-Myers Squibb Company; CereSpir, Inc.; Cogstate; Eisai Inc.; Elan Pharmaceuticals, Inc.; Eli Lilly and Company; EuroImmun; F. Hoffmann-La Roche Ltd and its affiliated company Genentech, Inc.; Fujirebio; GE Healthcare; IXICO Ltd.; Janssen Alzheimer Immunotherapy Research & Development, LLC.; Johnson & Johnson Pharmaceutical Research & Development LLC.; Lumosity; Lundbeck; Merck & Co., Inc.; Meso Scale Diagnostics, LLC.; NeuroRx Research; Neurotrack Technologies; Novartis Pharmaceuticals Corporation; Pfizer Inc.; Piramal Imaging; Servier; Takeda Pharmaceutical Company; and Transition Therapeutics. The Canadian Institutes of Health Research is providing funds to support ADNI clinical sites in Canada. Private sector contributions are facilitated by the Foundation for the National Institutes of Health (http://www.fnih.org). The grantee organization is the Northern California Institute for Research and Education, and the study is coordinated by the Alzheimer's Therapeutic Research Institute at the University of Southern California. ADNI data are disseminated by the Laboratory for Neuro Imaging at the University of Southern California.

Authors' disclosures available online (https://www.j-alz.com/manuscript-disclosures/18-0360r2).

REFERENCES

[1] Lin FV, Wang X, Wu R, Rebok GW, Chapman BP; Alzheimer's Disease Neuroimaging Initiative (2017) Identification of successful cognitive aging in the Alzheimer's Disease Neuroimaging Initiative Study. *J Alzheimers Dis* **59**, 101-111.

[2] Lin F, Ren P, Mapstone M, Meyers SP, Porsteinsson A, Baran TM, Alzheimer's Disease Neuroimaging Initiative (2017) The cingulate cortex of older adults with excellent memory capacity. *Cortex* **86**, 83-92.

[3] Mapstone M, Lin F, Nalls MA, Cheema AK, Singleton AB, Fiandaca MS, Federoff HJ (2017) What success can teach us about failure: The plasma metabolome of older adults with superior memory and lessons for Alzheimer's disease. *Neurobiol Aging* **51**, 148-155.

[4] Habib R, Nyberg L, Nilsson LG (2007) Cognitive and non-cognitive factors contributing to the longitudinal identification of successful older adults in the *Betula* study. *Neuropsychol Dev Cogn B Aging Neuropsychol Cogn* **14**, 257-273.

[5] Harrison TM, Weintraub S, Mesulam MM, Rogalski E (2012) Superior memory and higher cortical volumes in unusually successful cognitive aging. *J Int Neuropsychol Soc* **18**, 1081-1085.

[6] Sun FW, Stepanovic MR, Andreano J, Barrett LF, Touroutoglou A, Dickerson BC (2016) Youthful brains in older adults: Preserved neuroanatomy in the default mode and salience networks contributes to youthful memory in superaging. *J Neurosci* **36**, 9659-9668.

[7] Harrison TM, Maass A, Baker SL, Jagust WJ (2018) Brain morphology, cognition, and beta-amyloid in older adults with superior memory performance. *Neurobiol Aging* **67**, 162-170.

[8] Rogalski EJ, Gefen T, Shi J, Samimi M, Bigio E, Weintraub S, Geula C, Mesulam MM (2013) Youthful memory capacity in old brains: Anatomic and genetic clues from the Northwestern SuperAging Project. *J Cogn Neurosci* **25**, 29-36.

[9] Dekhtyar M, Papp KV, Buckley R, Jacobs HIL, Schultz AP, Johnson KA, Sperling RA, Rentz DM (2017) Neuroimaging markers associated with maintenance of optimal memory performance in late-life. *Neuropsychologia* **100**, 164-170.

[10] Wang X, Ren P, Baran TM, Raizada RDS, Mapstone M, Lin F; Alzheimer's Disease Neuroimaging Initiative (2017) Longitudinal functional brain mapping in supernormals. *Cereb Cortex*. doi: 10.1093/cercor/bhx322.

[11] Gefen T, Peterson M, Papastefan ST, Martersteck A, Whitney K, Rademaker A, Bigio EH, Weintraub S, Rogalski E, Mesulam MM, Geula C (2015) Morphometric and histologic substrates of cingulate integrity in elders with exceptional memory capacity. *J Neurosci* **35**, 1781-91.

[12] Sperling RA, Aisen PS, Beckett LA, Bennett DA, Craft S, Fagan AM, Iwatsubo T, Jr. CRJ, Kaye J, Montine TJ, Park DC, Reiman EM, Rowe CC, Siemers E, Stern Y, Yaffe K, Carrillo MC, Thies B, Morrison-Bogorad M, Wagster MV, Phelps CH (2011) Toward defining the preclinical stages of Alzheimer's disease: Recommendations from the National Institute on Aging-Alzheimer's Association workgroups on diagnostic guidelines for Alzheimer's disease. *Alzheimers Dement* **7**, 280-292.

[13] Crane PK, Carle A, Gibbons LE, Insel P, Mackin RS, Gross A, Jones RN, Mukherjee S, Curtis SM, Harvey D, Weiner M, Mungas D; Alzheimer's Disease Neuroimaging

Initiative (2012) Development and assessment of a composite score for memory in the Alzheimer's Disease Neuroimaging Initiative (ADNI). *Brain Imaging Behav* **6**, 502-516.

[14] Gibbons LE, Carle AC, Mackin RS, Harvey D, Mukherjee S, Insel P, Curtis SM, Mungas D, Crane PK; Alzheimer's Disease Neuroimaging Initiative (2012) A composite score for executive functioning, validated in Alzheimer's Disease Neuroimaging Initiative (ADNI) participants with baseline mild cognitive impairment. *Brain Imaging Behav* **6**, 517-527.

[15] Rossetti HC, Lacritz LH, Cullum CM, Weiner MF (2011) Normative data for the Montreal Cognitive Assessment (MoCA) in a population-based sample. *Neurology* **77**, 1272-1275.

[16] Jack CR, Jr., Wiste HJ, Weigand SD, Knopman DS, Mielke MM, Vemuri P, Lowe V, Senjem ML, Gunter JL, Reyes D, Machulda MM, Roberts R, Petersen RC (2015) Different definitions of neurodegeneration produce similar amyloid/neurodegeneration biomarker group findings. *Brain* **138**, 3747-59.

[17] Della Rosa PA, Cerami C, Gallivanone F, Prestia A, Caroli A, Castiglioni I, Gilardi MC, Frisoni G, Friston K, Ashburner J, Perani D; EADC-PET Consortium (2014) A standardized [^{18}F]-FDG-PET template for spatial normalization in statistical parametric mapping of dementia. *Neuroinformatics* **12**, 575-593.

[18] Desikan RS, Ségonne F, Fischl B, Quinn BT, Dickerson BC, Blacker D, Buckner RL, Dale AM, Maguire RP, Hyman BT, Albert MS, Killiany RJ (2006) An automated labeling system for subdividing the human cerebral cortex on MRI scans into gyral based regions of interest. *Neuroimage* **31**, 968-980.

[19] Saint-Aubert L, Barbeau EJ, Péran P, Nemmi F, Vervueren C, Mirabel H, Payoux P, Hitzel A, Bonneville F, Gramada R, Tafani M, Vincent C, Puel M, Dechaumont S, Chollet F, Pariente J (2013) Cortical florbetapir-PET amyloid load in prodromal Alzheimer's disease patients. *EJNMMI Res* **3**, 43.

[20] Landau S, Jagust W. Florbetapir processing methods, http://adni.loni.usc.edu/data-samples/access-data/, Last Updated December 3, 2015, Accessed on February 13, 2018.

[21] Landau S, Jagust W. UC Berkeley FDG MetaROI methods, http://adni.loni.usc.edu/data-samples/access-data/, Last Updated January 31, 2011, Accessed on February 13, 2018.

[22] Clifford R Jack J, Bennett DA, Blennow K, Carrillo MC, Dunn B, Haeberlein SB, Holtzman DM, Jagust W, Jessen F, Karlawish J, Liu E, Molinuevo JL, Montine T, Phelps C, Rankin KP, Rowe CC, Scheltens P, Siemers E, Snyder HM, Sperling R (2018) NIA-AA research framework: Toward a biological definition of Alzheimer's disease. *Alzheimers Dement* **14**, 535-562.

[23] Landau SM, Horng A, Fero A, Jagust WJ; Alzheimer's Disease Neuroimaging Initiative (2016) Amyloid negativity in patients with clinically diagnosed Alzheimer disease and MCI. *Neurology* **86**, 1377-1385.

[24] Joshi AD, Pontecorvo MJ, Clark CM, Carpenter AP, Jennings DL, Sadowsky CH, Adler LP, Kovnat KD, Seibyl JP, Arora A, Saha K, Burns JD, Lowrey MJ, Mintun MA, Skovronsky DM; Florbetapir F 18 Study Investigators (2012) Performance characteristics of amyloid PET with Florbetapir F 18 in patients with Alzheimer's disease and cognitively normal subjects. *J Nucl Med* **53**, 378-384.

[25] Jagust WJ, Landau SM, Shaw LM, Trojanowski JQ, Koeppe RA, Reiman EM, Foster NL, Petersen RC, Weiner MW, Price JC, Mathis CA; Alzheimer's Disease Neuroimaging Initiative (2009) Relationships between biomarkers in aging and dementia. *Neurology* **73**, 1193-1199.

[26] Moeller JR, Ishikawa T, Dhawan V, Spetsieris P, Mandel F, Alexander GE, Grady C, Pietrini P, Edielberg D (1996) The metabolic topography of normal aging. *J Cereb Blood Flow Metab* **16**, 385-398.

[27] Mormino EC, Betensky RA, Hedden T, Schultz AP, Amariglio RE, Rentz DM, Johnson KA, Sperling RA (2014) Synergistic effect of beta-amyloid and neurodegeneration on cognitive decline in clinically normal individuals. *JAMA Neurol* **71**, 1379-1385.

[28] Jack CR Jr, Therneau TM, Wiste HJ, Weigand SD, Knopman DS, Lowe VJ, Mielke MM, Vemuri P, Roberts RO, Machulda MM, Senjem ML, Gunter JL, Rocca WA, Petersen RC (2016) Transition rates between amyloid and neurodegeneration biomarker states and to dementia: A population-based, longitudinal cohort study. *Lancet Neurol* **15**, 56-64.

[29] Sperling RA, Johnson KA, Doraiswamy PM, Reiman EM, Fleisher AS, Sabbagh MN, Sadowsky CH, Carpenter A, Davis MD, Lu M, Flitter M, Joshi AD, Clark CM, Grundman M, Mintun MA, Skovronsky DM, Pontecorvo MJ; AV45-A05 Study Group (2013) Amyloid deposition detected with florbetapir F 18 (^{18} F-AV-45) is related to lower episodic memory performance in clinically normal older individuals. *Neurobiol Aging* **34**, 822-831.

[30] Fjell AM, McEvoy L, Holland D, Dale AM, Walhovd KB; Alzheimer's Disease Neuroimaging Initiative (2014) What is normal in normal aging? Effects of aging, amyloid and Alzheimer's disease on cerebral cortex and the hippocampus. *Prog Neurobiol* **117**, 20-40.

[31] Park DC, Reuter-Lorenz P (2009) The adaptive brain: Aging and neurocognitive scaffolding. *Annu Rev Psychol* **60**, 173-196.

[32] Leech R, Sharp DJ (2014) The role of the posterior cingulate cortex in cognition and disease. *Brain* **137**, 12-32.

[33] Buckner RL (2004) Memory and executive function in aging and AD: Multiple factors that cause decline and reserve factors that compensate. *Neuron* **44**, 195-208.

[34] Stern Y, Zarahn E, Habeck C, Holtzer R, Rakitin BC, Kumar A, Flynn J, Steffener J, Brown T (2008) A common neural network for cognitive reserve in verbal and object working memory in young but not old. *Cereb Cortex* **18**, 959-967.

[35] Seibert TM, Brewer JB (2011) Default network correlations analyzed on native surfaces. *J Neurosci Methods* **198**, 301-311.

[36] Zhu DC, Majumdar S, Korolev IO, Berger KL, Bozoki AC (2013) Alzheimer's disease and amnestic mild cognitive impairment weaken connections within the default-mode network: A multi-modal imaging study. *J Alzheimers Dis* **34**, 969-984.

[37] Jones DT, Machulda MM, Vemuri P, McDade EM, Zeng G, Senjem ML, Gunter JL, Przybelski SA, Avula RT, Knopman DS, Boeve BF, Petersen RC, Jack CR Jr (2011) Age-related changes in the default mode network are more advanced in Alzheimer disease. *Neurology* **77**, 1524-1531.

[38] Koch W, Teipel S, Mueller S, Benninghoff J, Wagner M, Bokde ALW, Hampel H, Coates U, Reiser M, Meindl T (2012) Diagnostic power of default mode network resting state fMRI in the detection of Alzheimer's disease. *Neurobiol Aging* **33**, 466-478.

[39] Sperling RA, LaViolette PS, O'Keefe K, O'Brien J, Rentz DM, Pihlajamaki M, Marshall G, Hyman BT, Selkoe DJ, Hedden T, Buckner RL, Becker JA, Johnson KA (2009) Amyloid deposition is associated with impaired default network function in older persons without dementia. *Neuron* **63**, 178-188.

[40] Mevel K, Chételat G, Eustache F, Desgranges B (2011) The default mode network in health aging and Alzheimer's disease. *Int J Alzheimers* **2011**, 535816.

[41] Liguori C, Chiaravalloti A, Sancesario G, Stefani A, Sancesario GM, Mercuri NB, Schillaci O, Pierantozzi M (2016) Cerebrospinal fluid lactate levels and brain [18F]FDG PET hypometabolism within the default mode network in Alzheimer's disease. *Eur J Nucl Med Mol Imaging* **43**, 2040-2049.

[42] Passow S, Specht K, Adamsen TC, Biermann M, Brekke N, Craven AR, Ersland L, Grüner R, Kleven-Madsen N, Kvernenes O-H, Schwarzlmüller T, Olesen RA, Hugdahl K (2015) Default-mode network functional connectivity is closely related to metabolic activity. *Hum Brain Mapp* **36**, 2027-2038.

[43] Hanseeuw BJ, Betensky RA, Schultz AP, Papp KV, Mormino EC, Sepulcre J, Bark JS, Cosio DM, LaPoint M, Chhatwal JP, Rentz DM, Sperling RA, Johnson KA (2017) Fluorodeoxyglucose metabolism associated with tau-amyloid interaction predicts memory decline. *Ann Neurol* **81**, 583-596.

[44] Pascoal TA, Mathotaarachchi S, Mohades S, Benedet AL, Chung CO, Shin M, Wang S, Beaudry T, Kang MS, Soucy J-P, Labbe A, Gauthier S, Rosa-Neto P (2017) Amyloid-beta and hyperphosphorylated tau synergy drives metabolic decline in preclinical Alzheimer's disease. *Mol Psychiatry* **22**, 306-311.

[45] Thal LJ, Kantarci K, Reiman EM, Klunk WE, Weiner MW, Zetterberg H, Galasko D, Praticó D, Griffin S, Schenk D, Siemers E (2006) The role of biomarkers in clinical trials for Alzheimer disease. *Alzheimer Dis Assoc Disord* **20**, 6-15.

[46] Craft S, Claxton A, Baker LD, Hanson AJ, Cholerton B, Trittschuh EH, Dahl D, Caulder E, Neth B, Montine TJ, Jung Y, Maldjian J, Whitlow C, Friedman S (2017) Effects of regular and long-acting insulin on cognition and Alzheimer's disease biomarkers: A pilot clinical trial. *J Alzheimers Dis* **57**, 1325-1334.

[47] Rogers J, Kirby LC, Hempelman SR, Berry DL, McGeer PL, Kaszniak AW, Zalinski J, Cofield M, Mansukhani L, Willson P, Kogan F (1993) Clinical trial of indomethacin in Alzheimer's disease. *Neurology* **43**, 1609.

[48] Ritchie CW, Bush AI, Mackinnon A, Macfarlane S, Mastwyk M, MacGregor L, Kiers L, Cherny R, Li Q-X, Tammer A, Carrington D, Mavros C, Volitakis I, Xilinas M, Ames D, Davis S, Bereuther K, Tanzi RE, Masters CL (2003) Metal-protein attenuation with iodochlorhydroxyquin (Clioquinol) targeting Abeta amyloid deposition and toxicity in Alzheimer disease: A pilot phase 2 clinical trial. *Arch Neurol* **60**, 1685-1691.

[49] Tuszynski MH, Thal L, Pay M, Salmon DP, U HS, Bakay R, Patel P, Blesch A, Vahlsing HL, Ho G, Tong G, Potkin SG, Fallon J, Hansen L, Mufson EJ, Kordower JH, Gall C, Conner J (2005) A phase 1 clinical trial of nerve growth factor gene therapy for Alzheimer disease. *Nat Med* **11**, 551-555.

[50] Ball K, Berch DB, Helmers KF, Jobe JB, Leveck MD, Marsiske M, Morris JN, Rebok GW, Smith DM, Tennstedt SL, Unverzagt FW, Willis SL (2002) Effects of cognitive training interventions with older adults: A randomized controlled trial. *JAMA* **288**, 2271-2281.

[51] Barnes DE, Yaffe K, Belfor N, Jagust WJ, DeCarli C, Reed BR, Kramer JH (2009) Computer-based cognitive training for mild cognitive impairment: Results from a pilot randomized, controlled trial. *Alzheimer Dis Assoc Disord* **23**, 205-210.

[52] Lin F, Heffner KL, Ren P, Tivarus ME, Brasch J, Chen D-G, Mapstone M, Porsteinsson AP, Tadin D (2016) Cognitive and neural effects of vision-based speed-of-processing training in older adults with amnestic mild cognitive impairment: A pilot study. *J AM Geriatr Soc* **64**, 1293-1298.